Letter

Decoherence-free many-body Hamiltonians in nonlinear waveguide quantum electrodynamics

Aviv Karnieli,[1,*] Offek Tziperman,[2] Charles Roques-Carmes,[1] and Shanhui Fan[1]
[1]*E. L. Ginzton Laboratories, Stanford University, 348 Via Pueblo, Stanford, California 94305, USA*
[2]*Technion–Israel Institute of Technology, Haifa 32000, Israel*

(Received 12 June 2024; accepted 19 November 2024; published 21 January 2025)

Enhancing interactions in many-body quantum systems, while protecting them from environmental decoherence, is at the heart of many quantum technologies. Waveguide quantum electrodynamics is a promising platform for achieving this, as it hosts infinite-range interactions and decoherence-free subspaces of quantum emitters. However, as coherent interactions between emitters are typically washed out in the wavelength-spacing regime hosting decoherence-free states, coherent control over the latter becomes limited, and many-body Hamiltonians in this important regime remain out of reach. Here we show that by incorporating emitter arrays with nonlinear waveguides hosting parametric gain, we obtain a unique class of many-body interaction Hamiltonians with coupling strengths that increase with emitter spacing, and persist even for wavelength-spaced arrays. We then propose to use these Hamiltonians to coherently generate decoherence-free states directly from the ground state, using only global squeezing drives, without the need for local addressing of individual emitters. Interestingly, we find that the dynamics approaches a unitary evolution in the limit of weak intrawaveguide squeezing, and we discuss potential experimental realizations of this effect. Our results pave the way towards coherent control protocols in waveguide quantum electrodynamics, with applications including quantum computing, simulation, memory, and nonclassical light generation.

DOI: 10.1103/PhysRevResearch.7.L012014

Introduction. Many-body quantum entanglement is a crucial resource for a plethora of quantum technologies, including quantum sensing [1], quantum simulation [2], and quantum computation [3]. Such schemes typically require strong interactions among system components, and the mitigation of environment-induced decoherence. One possible route for enhancing collective interactions is by engineering the environment to which the system is coupled [4–6]. For example, driving an emitter system with a squeezed bosonic reservoir can exponentially enhance interaction strength and cooperativity [7–10]. To mitigate interactions with the environment and subsequent decoherence, it is possible to prepare such systems in a decoherence-free (DF) subspace [11,12]. The DF subspace hosts many-body entangled states that are decoupled from the environment due to destructive interference of their decay pathways.

A promising platform for realizing many-body quantum entanglement is waveguide quantum electrodynamics (WQED) [13–17], wherein one-dimensional arrays of quantum emitters are coupled to a waveguide, acting as a continuous photonic reservoir. The one-dimensional geometry gives rise to infinite-range interactions mediated by the waveguide mode [17], which offers novel capabilities for quantum technologies [18–20] and fundamental investigations of correlated phenomena [21–24]. Reservoir engineering techniques in WQED utilizing a separately prepared squeezed vacuum drive have been proposed [25–27] for stabilizing steady states using strong dissipation. Furthermore, as WQED can be used to realize the Dicke model of superradiance for wavelength-spaced arrays [17], it supports a DF subspace, as explored in several theoretical [18,28–31] and experimental [32] investigations.

Despite these advancements, enhancement and protection of many-body correlations in WQED are still challenging. Since the DF subspace is inherently decoupled from the waveguide mode, accessing it often requires the local addressing of individual emitters [18,30–32], which, although feasible in platforms such as superconducting qubits, can still hamper scalability and fidelity [18]. Moreover, the coherent dynamics of the emitters is intrinsically limited in the wavelength-spacing regime hosting DF states, in which the many-body Hamiltonian vanishes [28]. This holds even if reservoir engineering schemes are employed [25–27], as the latter often rely on dissipation rather than on unitary evolution. Ultimately, these limitations hinder the realization of unitary dynamics and many-body Hamiltonians in this important regime of WQED.

In this letter, we lift these limitations by considering quantum emitter arrays coupled to *nonlinear* $\chi^{(2)}$ waveguides, serving as traveling-wave parametric amplifiers (or squeezers) [33–35]. Unlike squeezed-reservoir engineering, the parametric gain accumulation along the nonlinear waveguide in our system gives rise to an unconventional coherent atomic interaction that *increases* with interatomic distance, and it persists

*Contact author: karnieli@stanford.edu

Published by the American Physical Society under the terms of the Creative Commons Attribution 4.0 International license. Further distribution of this work must maintain attribution to the author(s) and the published article's title, journal citation, and DOI.

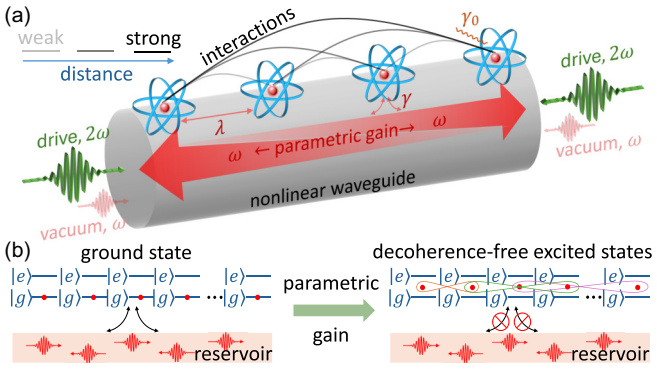

FIG. 1. Nonlinear waveguide quantum electrodynamics (WQED). (a) An array of N emitters is coupled to a $\chi^{(2)}$ nonlinear waveguide with coupling strength γ and decay into free space γ_0. The waveguide is driven by a classical field at 2ω, generating broadband parametric gain around frequency ω. Even when the emitters are evenly spaced by a wavelength, the parametric gain can still mediate coherent interactions between them, having the unusual property of increased interaction strength with increasing interatomic distance. (b) The parametric gain can coherently and globally drive the system from its ground state to decoherence-free excited states.

even in the wavelength-spacing regime. Surprisingly, we find that in the limit of weak intrawaveguide squeezing, the dynamics approaches an adiabatic unitary evolution under a many-body Hamiltonian, and the system can be coherently and globally driven to DF excited states directly from its ground state, without the need for local addressing of the emitters. We also investigate the emergent polaritonic excitations in the DF subspace, and we outline possible experimental WQED platforms. Our findings pave the way towards coherent control protocols in WQED, with applications ranging from quantum computation [18], memory [16], and simulation [20] to nonclassical light sources [24,36].

WQED with parametric gain. Our system comprises an array of N identical atoms with transition frequency ω, equally spaced by a distance Δz and coupled to a nonlinear waveguide of length L, as depicted in Fig. 1(a). The position of atom j is $z_j = z_1 + (j-1)\Delta z$ (where $0 \leqslant z_1 \leqslant z_j \leqslant z_N \leqslant L$), having a lowering (raising) operator $\sigma_{-,j}$ ($\sigma_{+,j}$). The waveguide is simultaneously driven by two counterpropagating classical pumps at a frequency of 2ω, driving a degenerate squeezing interaction that generates right- and left-propagating squeezed vacuum fields that gradually build up (amplified) along the propagation direction, with frequency ω, wave vector k, and group velocity v_g. We assume that the atoms are all coupled to the waveguide with equal rate $\gamma = \sqrt{2\pi g^2/v_g}$, where g is the coupling constant between the atoms and the waveguide field. The atoms can also have an external decay rate as a result of coupling to reservoirs other than the waveguide [γ_0 in Fig. 1(a)], leading to a coupling efficiency $\beta \equiv \gamma/(\gamma+\gamma_0) < 1$ [17]. We shall first consider the ideal case $\beta = 1$, and later discuss realistic experimental platforms with $\beta < 1$.

Denoting the right- and left-going interaction-picture field envelope operators by $A_s(z,t)$, with $s = \rightleftarrows$, the Hamiltonian of the total system is $H = H_{\mathrm{WQED}} + H_{\mathrm{NL}}$, where

$$H_{\mathrm{WQED}} = \hbar \sum_{s=\rightleftarrows} \int_{-\infty}^{\infty} dz\, A_s^\dagger(z)\left(-id_s v_g \frac{\partial}{\partial z}\right) A_s(z) + \hbar\sqrt{2\pi}\, g \sum_{s=\rightleftarrows} \sum_{j=1}^{N} [e^{d_s i k z_j} A_s(z_j)\sigma_{+,j} + \mathrm{H.c.}] \quad (1)$$

is the conventional Hamiltonian of WQED (with $d_{\rightleftarrows} = \pm 1$), and

$$H_{\mathrm{NL}} = \hbar \sum_{s=\rightleftarrows} \left[\kappa_s \int_0^L A_s(z) A_s(z) dz + \mathrm{H.c.}\right] \quad (2)$$

is the nonlinear Hamiltonian for the waveguide field, where $\kappa_{\rightleftarrows}$ denote the nonlinear coupling parameters, proportional to the waveguide's nonlinearity and to the strength of the pump fields at 2ω. The addition of the quadratic nonlinear Hamiltonian introduces parametric gain accumulation (squeezing) for the fields propagating along the waveguide.

We show in the Supplemental Material (SM) sections S1–S2 [37] that the fields at atomic positions z_j and time t can be written in terms of a Bogoliubov transformation of the retarded input fields $A_{\rightarrow}(0, t - z_j/v_g)$ and $A_{\leftarrow}(L, t - (L - z_j)/v_g)$, assumed to be in the vacuum state. Under the Markovian approximation (assuming the atomic chain is not too long such that retardation could be neglected, $v_g/L \gg \gamma$ [15]), the dynamics of the atomic system can be obtained using the SLH formalism [38]. The system evolves under the Lindblad master equation

$$\dot{\rho} = -\frac{i}{\hbar}[H, \rho] + \sum_{s=\rightleftarrows} \mathcal{D}_{L_s}[\rho], \quad (3)$$

with L_s denoting the SLH jump operators, and $\mathcal{D}_X[\rho] = X\rho X^\dagger - 1/2\{X^\dagger X, \rho\}$ denotes the dissipator corresponding to a jump operator X.

The most general form of the resulting Hamiltonian and jump operators is given in the SM section S3 [37]. Hereafter, we make the following assumptions: (i) wavelength spacing of the array $\Delta z = m\lambda$, with m being an integer and $\lambda = 2\pi/k$ (similar conclusions hold under the more general Bragg condition $\Delta z = m\lambda/2$); (ii) $z_1 = 0$ and $z_N = L$, i.e., the atom array and the nonlinear region of the waveguide coincide; and (iii) symmetric pump fields and nonlinearity: ensuring the same squeezing gain and phase for the right- and left-propagating fields. Denoting by r and θ the total squeeze parameter and phase, respectively, the accumulated squeeze parameters from the right and left, up to atom j, are written, respectively, as $r_{\rightarrow,j} = r(j-1)/(N-1)$ and $r_{\leftarrow,j} = r(N-j)/(N-1)$. Under these assumptions, we find

$$H = \frac{\gamma}{2} \sum_{i,j=1}^{N} \sinh\left(\frac{r|i-j|}{N-1}\right)(e^{-i\theta}\sigma_{+,j}\sigma_{+,i} + e^{i\theta}\sigma_{-,j}\sigma_{-,i}),$$

$$L_s = \sqrt{\gamma} \sum_{j=1}^{N} (\cosh r_{s,j}\sigma_{-,j} - ie^{-i\theta} \sinh r_{s,j}\sigma_{+,j}). \quad (4)$$

Interestingly, the interaction Hamiltonian in Eq. (4) persists even though the atoms are spaced by a wavelength. In contrast, in the absence of parametric gain in the waveguide under

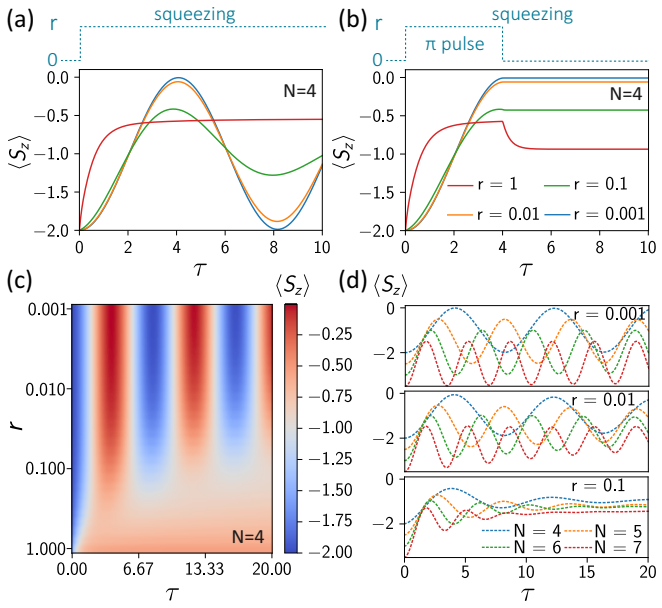

FIG. 2. Emergence of coherent dynamics under weak parametric gain. The evolution of the global population is plotted for different squeezing parameters r and emitter number N. Whereas for $r = 1$ the dynamics is completely dissipative, coherent Rabi oscillations emerge for $r \ll 1$. (a), (b) $N = 4$ atoms. For $r \ll 1$, the population remains excited even after the squeezing is turned off [e.g., when the squeezing drive is a π-pulse as in (b)] and does not decay back to the reservoir: a signature of decoherence-free states. (c) Oscillations for $N = 4$ atoms and a continuous change in squeezing parameter. (d) Oscillations for different atom numbers N and varying squeezing levels, where the Rabi frequency increases with N. All plots assume $\beta = 1$.

the same conditions, coherent interatomic interactions are washed out and the dynamics is purely dissipative (the Dicke-superradiant regime) [28]. The Hamiltonian demonstrates an unusual property of interaction strength that is *exponentially increasing* with increased interatomic distance. This peculiar feature stems from the amplification of photons mediating the interaction between distant atoms. While exponential-range coupling was previously considered in atomic simulators with treelike geometry [39,40], our Hamiltonian involves an all-to-all connectivity, courtesy of the waveguide mode. Furthermore, unlike the conventional spin-exchange interaction, here each pairwise interaction term has the form of a two-axis twisting Hamiltonian with a separation-dependent coupling [41,42]. Thus, the proposed system can realize even more diverse forms of spin squeezing and quantum simulation.

To assess the dynamical features of our system in the wavelength-spacing regime, in Figs. 2(a)–2(c) we plot the expectation value of the global population operator $S_z = \sum_i \sigma_{z,i}$ for $N = 4$ quantum emitters starting from the global ground state ($\langle S_z \rangle = -N/2$) for different levels of squeezing. When $r \sim 1$, the system is quickly stabilized to a steady state through dissipation. However, when $r \ll 1$, coherent Rabi oscillations emerge, displaying increasing visibility for weaker squeezing. When varying the squeezing parameter, we rescaled the time to $\tau = \gamma r t$. As we show below, γr is the universal scale of the emergent adiabatic oscillations, which become slower for decreasing r. The continuous transition between complete dissipation and coherent oscillations as a function of r and τ is plotted in Fig. 2(c), and Fig. 2(d) displays Rabi oscillations for $4 \leqslant N \leqslant 7$ and select values of r, where Rabi frequency increases with N. Richer dynamics for $N \geqslant 8$, comprising several Rabi frequencies, is discussed in a later section, and also in SM, section S7 [37]. Interestingly, as shown in Fig. 2(b), if the squeezing drive is turned off, the emitter population does not decay: this is a manifestation of the excitation of DF states.

Decoherence-free subspace and coherent adiabatic dynamics. In the Dicke regime of conventional WQED, permutation symmetry allows us to express the dynamics in terms of the collective operators $S_\pm = \sum_i \sigma_{\pm,i}$ and S_z. The commutation of $S^2 = S_z^2 + \{S_+, S_-\}/2$ with the Hamiltonian and all jump operators then ensures [43] that the Lindbladian can be block-diagonalized into subspaces of total angular momentum $j = 0, (1/2), 1, (3/2), \ldots, N/2$ for even (odd) N, as depicted in Fig. 3(a). The DF subspace contains all states that are annihilated by S_-, which are the (possibly degenerate) states of the form $m = -j$, where $-j \leqslant m \leqslant j$ is the z-component quantum number of the total angular momentum.

In the presence of permutation symmetry, DF states do not couple with one another, as they reside in different j-subspaces. In particular, the global ground state (experimentally, the system can be prepared in the global ground state by thermalization, laser cooling, or coherent initialization) $|gg\cdots g\rangle$ with $j = N/2$ and $m = -N/2$ is decoupled from other excited states ($j = -m > N/2$) in the DF subspace. The nonlinear parametric gain allows one to break permutation symmetry [as in Eq. (4)], without the need for local addressing of individual emitters [18,30–32]. As such, different j-subspaces can now be dynamically coupled via global driving, and as a result, so can DF states.

In fact, in the weak-squeezing limit $r \ll 1$ of Eq. (4), it can be shown that the dynamics involves *only* DF states. As can be seen in Fig. 3(b), for $r \ll 1$ the state resides exclusively in the DF subspace. To understand this, consider the projection operator onto the DF subspace, $\mathcal{H}_P$, denoted as P (and its superoperator version $\mathcal{P}$, such that $\mathcal{P}\rho = P\rho P$). Writing an arbitrary state ρ as $\rho = \mathcal{P}\rho + (1 - \mathcal{P})\rho$, and inspecting the dynamics of $\mathcal{P}\rho$ and $(1 - \mathcal{P})\rho$, we show in SM section S5 [37] that bright states $(1 - \mathcal{P})\rho$ experience superradiant decay with rate $\sim\gamma N$ back into the DF subspace. On the other hand, we find that the dynamics of DF states $\mathcal{P}\rho$ occurs at a much slower rate $\sim r\gamma \ll N\gamma$.

Remarkably, we further find that the evolution of the DF states can be arbitrarily close to a unitary for $N \geqslant 4$ atoms. As we show in SM section S5 [37], the dissipative part of the slow dynamics within $\mathcal{H}_P$ occurs at ultraslow rates $\sim r^2\gamma$, whereas the coherent part evolves with a rate $\sim r\gamma$ [see arrows in Fig. 3(a)]. This means that we should be expecting Rabi oscillations with a relatively long coherence time, with $\sim 1/2r$ visible periods. Thus, in the weak squeezing limit, and to first order in r, the dynamics approaches a unitary evolution (as can be seen in Fig. 2), wherein $H \to PHP$, corresponding to quantum Zeno dynamics [6,18]. For the case of two and three atoms, $PHP = 0$, such that the dynamics is completely dissipative (with rate $\sim r^2\gamma$).

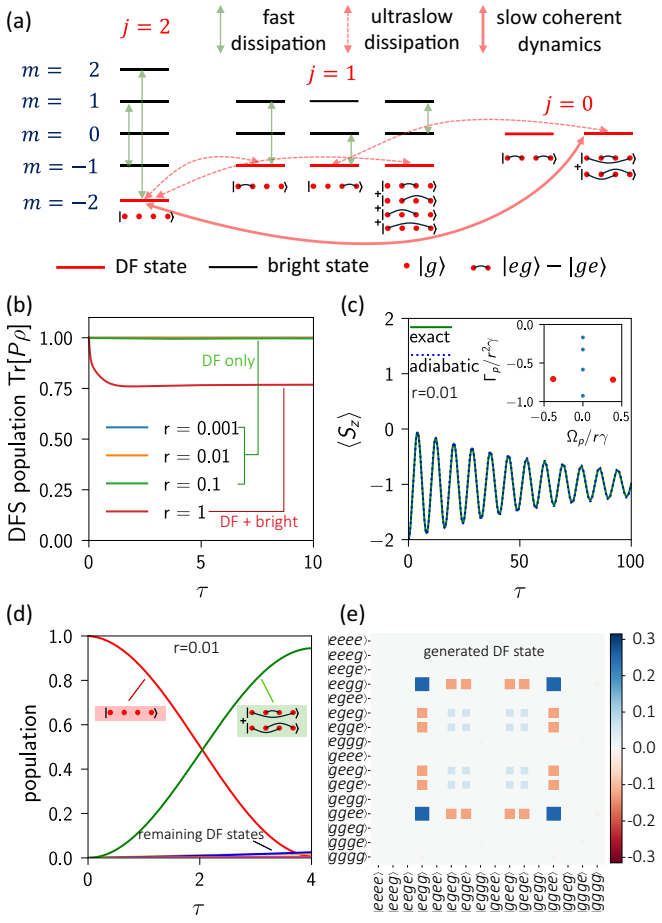

FIG. 3. Coherent adiabatic dynamics in the decoherence-free subspace. (a) Total angular momentum subspaces j (here illustrated for four atoms). Each j-subspace hosts DF states with total z-component $m = -j$, comprising antisymmetric dimer states [44]. The parametric gain breaks permutation symmetry, thus coupling different j subspaces. Fast dissipation of bright states $\sim\gamma$ can then be adiabatically eliminated, leaving slow coherent dynamics between DF states with rate $\sim r\gamma$, as well as ultraslow dissipation $\sim r^2\gamma$. (b) Projection of the state ρ onto the DF subspace $\mathcal{H}_P$ indeed shows that for $r \ll 1$, all populated states are decoherence-free. (c) Exact and adiabatically eliminated dynamics, resembling a finite-lifetime polariton. Inset: eigenvalues of $H_{\rm eff}$ on the complex plain (polariton energies highlighted). (d) DF state populations along a half Rabi cycle, converting between the global ground state and the entangled $j = 0$ DF state with a fidelity of 94.5% (which improves with decreasing r). (e) Density matrix of the generated state in (d). All plots assume $\beta = 1$.

These observations motivate the adiabatic elimination [45] of the fast dynamics of bright states, leaving us with an adiabatic Hamiltonian and jump operators $H_{\rm ad}$, $\{L_{{\rm ad},i}\}$ that act on states in $\mathcal{H}_P$ alone. We outline the adiabatic elimination procedure in SM section S6 [37], which for general open quantum systems can be performed numerically in terms of Liouville superoperators. We find that our adiabatically eliminated dynamics hosts polaritonic excitations within the DF subspace, which are the eigenstates of the non-Hermitian effective Hamiltonian $H_{\rm eff} = H_{\rm ad} - i\frac{1}{2}\sum_i L^\dagger_{{\rm ad},i}L_{{\rm ad},i}$. These polaritonic eigenstates may in general have complex eigenfrequencies $\Omega_p + i\Gamma_p$, with $\Gamma_p \leqslant 0$, where $\Omega_p \sim r\gamma$ and $\Gamma_p \sim r^2\gamma$. Figure 3(c) shows the time evolution of $\langle S_z\rangle$ under the exact [Eq. (4)] and adiabatically eliminated dynamics for $N = 4$, where the inset shows the complex eigenvalues of the DF-subspace polaritons. While polaritons in the DF subspace have a finite coherence time due to ultraslow dissipation and dephasing in $\mathcal{H}_p$, we stress that when the squeezing drive is turned off (at any finite time t_0), so does this dissipation; one is left with a DF state that does not decay for $t \geqslant t_0$ [see Fig. 2(b)]. In this manner, we show in Figs. 3(d) and 3(e) that one can adiabatically generate DF excited states directly from the global ground state. Such states can be highly entangled, as can be seen in the Hinton diagram of the corresponding density matrix in Fig. 3(e).

Comparison with squeezed reservoir engineering. Squeezed reservoir engineering in WQED has been theoretically proposed [25–27] for the stabilization of steady-state dark states and spin squeezing using a separately prepared squeezed vacuum. In these schemes, however, there is no parametric gain accumulation between the emitters, and the permutation symmetry is not broken. In SM section S5 [37], we use our formalism to derive the reservoir engineering (RE) Hamiltonian and jump operators in the regime where the spacing between the emitter is comparable to the wavelength. Setting (without loss of generality) $\theta = -\pi/2$ and denoting by $\bar{r}$ the squeeze parameter of the separately prepared squeezed vacuum, we find $H_{\rm RE} = 0$ and $L^{\rightarrow}_{\rm RE} = L^{\leftarrow}_{\rm RE} = \sqrt{\gamma}(\cosh\bar{r}S_- + \sinh\bar{r}S_+)$, where $S_\pm = \sum_j \sigma_{\pm,j}$ are the global raising and lowering operators. Note that since $H_{\rm RE} = 0$, the RE dynamics in the wavelength-spacing regime is completely dissipative. Further, since the jump operators are permutationally symmetric (and both commute with S^2), the dynamics cannot couple different total angular momentum subspaces [the j-subspaces of Fig. 3(a)], and thus cannot couple between different decoherence-free states. Our proposal, on the other hand, allows for a unitary evolution, which also couples between different j-subspaces by breaking permutation symmetry.

Experimental considerations. While DF states are immune to dissipation into the waveguide reservoir (modeled by the jump operator S_-), they are still susceptible to other types of decoherence, such as radiative loss outside the waveguide, qubit dephasing, and thermal noise (which are modeled by different classes of jump operators), while their dynamics can be sensitive to disorder in the qubit frequencies and positioning. Further, as with other adiabatic schemes in WQED [18], one needs to ensure that the total decoherence rate is slower than the rate of the adiabatic dynamics. In our case, observing the predicted Rabi oscillations of DF states amounts to requiring that $r \ll 1$ and $1 - \beta \ll r$ (ideally, $1 - \beta \sim r^2$), which implies near-ideal coupling efficiency $\beta \simeq 1$. Similarly, as we show in SM section S9 [37], the effect of finite-temperature of the waveguide system has a similar signature on decoherence. We require that, in the limit $r \ll 1$, the rate of thermal decoherence $\sim\gamma\bar{n}_{\rm th}$ (where $\bar{n}_{\rm th}$ is the thermal photon occupation number) is much slower than the rate of adiabatic oscillations, $\bar{n}_{\rm th} \ll r$ (ideally, $\bar{n}_{\rm th} \sim r^2$).

Figure 4 summarizes the effects of nonideal system parameters on the dynamics of our model. In Fig. 4(a) we plot the

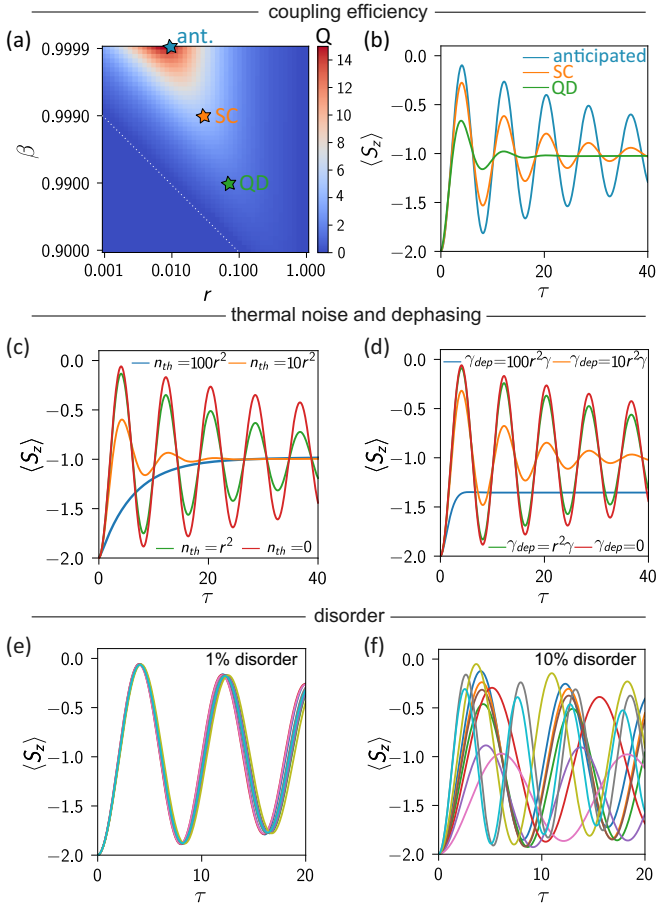

FIG. 4. Experimental considerations in realistic WQED platforms. (a), (b) Effect of coupling efficiency. Coherent adiabatic oscillations $\sim r\gamma$ must be faster than the radiative decay rate $\gamma_0 = [(1-\beta)/\beta]\gamma$, ideally with $1-\beta \sim r^2$. (a) Polaritonic quality factor $Q = \Omega_p/2\Gamma_p$ for $N = 4$ atoms. Onset of oscillations $1-\beta = r$ shown by a dashed white line. State-of-the-art values of $\beta = 0.99$ for quantum dots (QDs) [17,46] and $\beta = 0.999$ superconducting qubits (SCs) [17,47] are shown at the maximal Q value. (b) Dynamics with finite $1-\beta$ values corresponding to the marked points in (a): $\beta = 0.99,\ 0.999,\ 0.9999$, and $r = 0.086,\ 0.025,\ 0.01$, respectively. (c) Effect of thermal noise with average photon number $n_{\rm th}$ and (d) individual qubit dephasing (with rate $\gamma_{\rm dep}$). (e), (f) Effect of phase and gain disorder. Ten different realizations of random Gaussian disorder, where the indicated percentages are relative to r (the scale of the slow dynamics) and correspond to the standard deviation in the simulation. In (c)–(f), $N = 4$ and $r = 0.01$.

DF polariton quality factors $Q = |\Omega_p/2\Gamma_p|$ as a function of squeezing parameter r and coupling efficiency β. The onset of Rabi oscillations (the line $1-\beta = r$) is also shown. Considering the state-of-the-art values for two different WQED platforms [17], quantum dots (QDs) with $\beta = 0.99$ [17,46,48] and superconducting (SC) qubits with $\beta = 0.999$ [17,47], we plot in Fig. 4(b) the corresponding dynamics with the ideal r value for each case, as indicated in Fig. 4(a). Anticipating future improvements of coupling efficiency, we also plot the nearly ideal case of $\beta = 0.9999$ and $r = 0.01$ ($1-\beta \sim r^2$), for which loss is commensurate with the ultraslow DF polariton dissipation. The effect of thermal noise is depicted in Fig. 4(c), where we note that the required level of thermal occupation number in this example, $\bar{n}_{\rm th} \sim r^2 \sim 10^{-4}$, has already been realized experimentally for superconducting qubits [49,50]. The effect of individual qubit dephasing with rate $\gamma_{\rm dep}$ is depicted in Fig. 4(d), with a similar requirement on the dephasing rate ideally being $\gamma_{\rm dep} \sim r^2\gamma$.

Finally, Figs. 4(e) and 4(f) depict the effect of phase and gain disorder, relative to the adiabatic oscillation scale $\sim r$ of the ordered Hamiltonian. This can be caused, e.g., by disorder in emitter frequencies and positioning. Subradiant and decoherence-free states are known to be sensitive to such disorder, causing deviation from the Bragg-spacing condition [17]. In our context, disorder can affect the structure of the interaction Hamiltonian, thus affecting the dynamics. For superconducting qubits, keeping the relative disorder below 1% (in units of r, e.g., below 10^{-4} for $r = 0.01$) requires control of the qubit resonance with sub-MHz resolution. This is possible with frequency-tunable transmon qubits [51], as was also recently demonstrated in WQED [52].

To conclude, with the current parameters of WQED platforms, there is still room for improvement to push this scheme to its full potential and making it scalable, a challenge shared by WQED hardware in general. Proof-of-concept realization of our scheme in the SC and QD platforms can nonetheless still be pursued. For example, this can be done by integrating the emitters into traveling-wave parametric amplifiers. With the advent of SC Josephson amplifiers [33,34,53] and integrated nonlinear optical waveguides (e.g., $\chi^{(2)}$ platforms such as lithium niobate [35]), we believe that an experimental proof-of-concept is within reach. Moreover, as our proposal requires a lower level of intrawaveguide squeezing, other platforms can prove to be relevant.

Dynamics of larger systems. We now further investigate how these observations generalize and become more complex for larger numbers of emitters. Figure 5(a) shows that the dynamics for emitter numbers $N \geqslant 8$ becomes richer and involves several Rabi frequencies [compare with Fig. 2(d) for $N < 8$]. The reason for the richer behavior for $N \geqslant 8$ is the interplay of additional $j-$DFSs that are now coupled by the Hamiltonian. This is illustrated in Fig. 5(b). Our Hamiltonian couples different j-subspaces that differ by two excitations (i.e., two spin-1/2 flips). For $N < 8$ [shaded box in Fig. 5(b)], there exists only one subspace that couples to the state $|gg\cdots g\rangle$, which serves as the initial condition in our simulations. The state $|gg\cdots g\rangle$ resides in the subspace $j = N/2$, and the Hamiltonian always couples this state to a single state in the subspace $j = N/2-2$ (which could possibly form a superposition of the basis states of that subspace). Thus, for $N < 8$, we observe Rabi oscillations between $|gg\cdots g\rangle$ and the single state in $j = N/2-2$. For $N \geqslant 8$ [unshaded box in Fig. 5(b)], there are now additional j-subspaces that can connect to $|gg\cdots g\rangle$ via many different intermediate states. We can thus expect beating between many different Rabi frequencies. These observations are also illustrated in Figs. 5(c) and 5(d), comparing the distribution of the complex eigenvalues of the effective Hamiltonian for $N = 7$ and 8, color-coded by the overlap of their corresponding eigenstates with the state $|gg\cdots g\rangle$: while there exists only a pair of such eigenstates

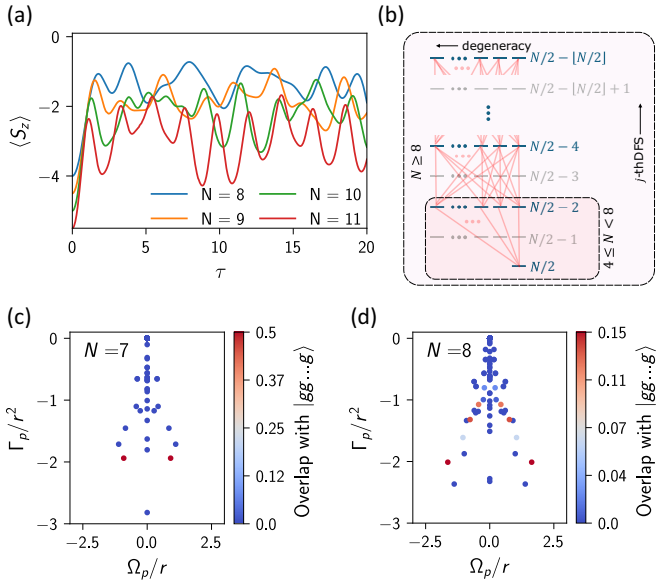

FIG. 5. Dynamics of larger systems. (a) For $N \geqslant 8$, the evolution of the system from the state $|gg\cdots g\rangle$ becomes richer, as can be observed in the population dynamics (here, $r = 0.001$). (b) The reason for this lies in the way the Hamiltonian couples different j-DFSs. Here, we use red lines to partially depict the couplings between even-excitation-number DFSs (blue), but we stress that couplings also exist between the odd-excitation-number DFSs (gray). For $4 \leqslant N < 8$, the $j = N/2$ DFS can only couple to the $j = N/2 - 2$ DFS, facilitating only a single pair of eigenstates that involve $|gg\cdots g\rangle$ [red dots in panel (c)]; for $N \geqslant 8$ DFSs with higher j (and increasing degeneracy) can couple, and more eigenstates overlapping with $|gg\cdots g\rangle$ are formed [color-coded dots in panel (d)]. (c), (d) Complex eigenvalue maps of H_{eff} for (c) $N = 7$ and (d) $N = 8$. Color-code represents the overlap of the corresponding eigenstates with $|gg\cdots g\rangle$.

for $N = 7$, corresponding to one Rabi frequency, there are multiple pairs of eigenstates for $N = 8$, each corresponding to a different Rabi oscillation, which explains the complex dynamics shown in Fig. 5(a).

Discussion and outlook. We have shown that coupling atom arrays to nonlinear waveguides hosting parametric gain leads to a unique coherent interatomic interaction in a regime where such interactions are typically washed out. We have further shown how this dynamics approaches unitary evolution within the DF subspace, and it can be used to generate entangled DF states directly from the ground state using only global drives.

Unlike dissipative reservoir engineering schemes with squeezed vacuum [25–27] (see also SM section S4 [37]), our proposal utilizes an emergent coherent many-body Hamiltonian interaction to dynamically steer desired atomic states. As the coherent dynamics becomes richer for larger atom numbers (Fig. 5 and SM section S7 [37]), further work is needed to discover universal coherent control schemes over arbitrarily large DF states using global parametric driving. In particular, it will be intriguing to extend previous proposals for DF quantum computation in WQED [18], relying on individual qubit driving to implement quantum gates, to allow for globally driven quantum gates, with a potential reduction in noise and improvement of gate fidelity. This, however, will require further analysis beyond the scope of the current work, such as a proof of universality and a proper choice of qubit encoding. One possible route to achieve these goals is to employ time-dependent [54] and spectrally shaped [55] drives, as well as globally controlled waveguide dispersion [56,57]. The gradual formation of such DF states can then be probed by photon scattering [16,31,58–60]. It would be intriguing to also consider other forms of nonlinearity leading to exotic physics in WQED, as proposed using Kerr cavity arrays [61,62].

The unique nonlocal structure of our interaction Hamiltonian Eq. (4) may prove useful for implementing quantum simulations [39,40], topological squeezing-based models [63], as well as spin-squeezing with distance-dependent coupling [64]. The possibility to drive DF states can be useful in quantum thermodynamic applications in WQED [65], such as energy storage in quantum batteries [66]. Finally, selective releasing of excitations stored in the DF states back into the waveguide may enable novel schemes for on-demand, macroscopic nonclassical light sources [16,24].

Acknowledgments. A.K. is supported by the VATAT-Quantum fellowship by the Israel Council for Higher Education; the Urbanek-Chodorow postdoctoral fellowship by the Department of Applied Physics at Stanford University; the Zuckerman STEM leadership postdoctoral program; and the Viterbi fellowship by the Technion. C.R.-C. is supported by a Stanford Science Fellowship. S.F. acknowledges the support from the Department of Energy (Grant No. DE-FG02-07ER46426). The authors acknowledge fruitful discussions with Janet Zhong, Dr. Renwen Yu, Dr. Nicholas Rivera, and Dr. Eric Rosenthal.

The authors declare no conflict of interest.

Data Availability. Data may be obtained from the authors upon reasonable request.

[1] C. L. Degen, F. Reinhard, and P. Cappellaro, Quantum sensing, Rev. Mod. Phys. **89**, 035002 (2017).

[2] I. M. Georgescu, S. Ashhab, and F. Nori, Quantum simulation, Rev. Mod. Phys. **86**, 153 (2014).

[3] M. A. Nielsen and I. L. Chuang, *Quantum Computation and Quantum Information* (Cambridge University Press, Cambridge, UK, 2010).

[4] J. F. Poyatos, J. I. Cirac, and P. Zoller, Quantum reservoir engineering with laser cooled trapped ions, Phys. Rev. Lett. **77**, 4728 (1996).

[5] D. Kienzler, H. Y. Lo, B. Keitch, L. De Clercq, F. Leupold, F. Lindenfelser, M. Marinelli, V. Negnevitsky, and J. P. Home, Quantum harmonic oscillator state synthesis by reservoir engineering, Science **347**, 53 (2015).

[6] P. M. Harrington, E. J. Mueller, and K. W. Murch, Engineered dissipation for quantum information science, Nat. Rev. Phys. **4**, 660 (2022).

[7] W. Qin, A. Miranowicz, P. B. Li, X. Y. Lü, J. Q. You, and F. Nori, Exponentially enhanced light-matter interaction, cooperativities, and steady-state entanglement using parametric amplification, Phys. Rev. Lett. **120**, 093601 (2018).

[8] C. Leroux, L. C. Govia, and A. A. Clerk, Enhancing cavity quantum electrodynamics via antisqueezing: Synthetic ultrastrong coupling, Phys. Rev. Lett. **120**, 093602 (2018).

[9] S. Zeytinoglu, A. Imamoglu, and S. Huber, Engineering matter interactions using squeezed vacuum, Phys. Rev. X **7**, 021041 (2017).

[10] S. C. Burd, R. Srinivas, H. M. Knaack, W. Ge, A. C. Wilson, D. J. Wineland, D. Leibfried, J. J. Bollinger, D. T. Allcock, and D. H. Slichter, Quantum amplification of boson-mediated interactions, Nat. Phys. **17**, 898 (2021).

[11] D. A. Lidar, I. L. Chuang, and K. B. Whaley, Decoherence-free subspaces for quantum computation, Phys. Rev. Lett. **81**, 2594 (1998).

[12] P. Zanardi and M. Rasetti, Noiseless quantum codes, Phys. Rev. Lett. **79**, 3306 (1997).

[13] J. T. Shen and S. Fan, Coherent photon transport from spontaneous emission in one-dimensional waveguides, Opt. Lett. **30**, 2001 (2005).

[14] J. T. Shen and S. Fan, Theory of single-photon transport in a single-mode waveguide. I. Coupling to a cavity containing a two-level atom, Phys. Rev. A **79**, 023837 (2009).

[15] T. Caneva, M. T. Manzoni, T. Shi, J. S. Douglas, J. Ignacio Cirac, and D. E. Chang, Quantum dynamics of propagating photons with strong interactions: A generalized input–output formalism, New J. Phys. **17**, 113001 (2015).

[16] A. Asenjo-Garcia, M. Moreno-Cardoner, A. Albrecht, H. J. Kimble, and D. E. Chang, Exponential improvement in photon storage fidelities using subradiance and "selective radiance" in atomic arrays, Phys. Rev. X **7**, 031024 (2017).

[17] A. S. Sheremet, M. I. Petrov, I. V. Iorsh, A. V. Poshakinskiy, and A. N. Poddubny, Waveguide quantum electrodynamics: Collective radiance and photon-photon correlations, Rev. Mod. Phys. **95**, 015002 (2023).

[18] V. Paulisch, H. J. Kimble, and A. González-Tudela, Universal quantum computation in waveguide QED using decoherence free subspaces, New J. Phys. **18**, 043041 (2016).

[19] D. Malz and J. I. Cirac, Nondestructive photon counting in waveguide QED, Phys. Rev. Res. **2**, 033091 (2020).

[20] C. Tabares, A. Muñoz De Las Heras, L. Tagliacozzo, D. Porras, and A. González-Tudela, Variational quantum simulators based on waveguide QED, Phys. Rev. Lett. **131**, 073602 (2023).

[21] A. Goban, C. L. Hung, J. D. Hood, S. P. Yu, J. A. Muniz, O. Painter, and H. J. Kimble, Superradiance for atoms trapped along a photonic crystal waveguide, Phys. Rev. Lett. **115**, 063601 (2015).

[22] Y. X. Zhang and K. Mølmer, Theory of subradiant states of a one-dimensional two-level atom chain, Phys. Rev. Lett. **122**, 203605 (2019).

[23] A. V. Poshakinskiy, J. Zhong, Y. Ke, N. A. Olekhno, C. Lee, Y. S. Kivshar, and A. N. Poddubny, Quantum Hall phases emerging from atom–photon interactions, npj Quantum Inf. **7**, 34 (2021).

[24] O. Tziperman, G. Baranes, A. Gorlach, R. Ruimy, C. Mechel, M. Faran, N. Gutman, A. Pizzi, and I. Kaminer, The quantum state of light in collective spontaneous emission, arXiv:2306.11348.

[25] J. You, Z. Liao, S. W. Li, and M. S. Zubairy, Waveguide quantum electrodynamics in squeezed vacuum, Phys. Rev. A **97**, 023810 (2018).

[26] S. Y. Bai and J. H. An, Generating stable spin squeezing by squeezed-reservoir engineering, Phys. Rev. Lett. **127**, 083602 (2021).

[27] R. Gutiérrez-Jáuregui, A. Asenjo-Garcia, and G. S. Agarwal, Dissipative stabilization of dark quantum dimers via squeezed vacuum, Phys. Rev. Res. **5**, 013127 (2023).

[28] A. Albrecht, L. Henriet, A. Asenjo-Garcia, P. B. Dieterle, O. Painter, and D. E. Chang, Subradiant states of quantum bits coupled to a one-dimensional waveguide, New J. Phys. **21**, 025003 (2019).

[29] A. F. Kockum, G. Johansson, and F. Nori, Decoherence-free interaction between giant atoms in waveguide quantum electrodynamics, Phys. Rev. Lett. **120**, 140404 (2018).

[30] H. Pichler, T. Ramos, A. J. Daley, and P. Zoller, Quantum optics of chiral spin networks, Phys. Rev. A **91**, 042116 (2015).

[31] R. Holzinger, R. Gutiérrez-Jáuregui, T. Hönigl-Decrinis, G. Kirchmair, A. Asenjo-Garcia, and H. Ritsch, Control of localized single- and many-body dark states in waveguide QED, Phys. Rev. Lett. **129**, 253601 (2022).

[32] M. Zanner, T. Orell, C. M. Schneider, R. Albert, S. Oleschko, M. L. Juan, M. Silveri, and G. Kirchmair, Coherent control of a multi-qubit dark state in waveguide quantum electrodynamics, Nat. Phys. **18**, 538 (2022).

[33] C. Macklin, K. O'Brien, D. Hover, M. E. Schwartz, V. Bolkhovsky, X. Zhang, W. D. Oliver, and I. Siddiqi, A near-quantum-limited Josephson traveling-wave parametric amplifier, Science **350**, 307 (2015).

[34] J. Y. Qiu, A. Grimsmo, K. Peng, B. Kannan, B. Lienhard, Y. Sung, P. Krantz, V. Bolkhovsky, G. Calusine, D. Kim, A. Melville, B. M. Niedzielski, J. Yoder, M. E. Schwartz, T. P. Orlando, I. Siddiqi, S. Gustavsson, K. P. O'Brien, and W. D. Oliver, Broadband squeezed microwaves and amplification with a Josephson travelling-wave parametric amplifier, Nat. Phys. **19**, 706 (2023).

[35] R. Nehra, R. Sekine, L. Ledezma, Q. Guo, R. M. Gray, A. Roy, and A. Marandi, Few-cycle vacuum squeezing in nanophotonics, Science **377**, 1333 (2022).

[36] A. González-Tudela, V. Paulisch, D. E. Chang, H. J. Kimble, and J. I. Cirac, Deterministic generation of arbitrary photonic states assisted by dissipation, Phys. Rev. Lett. **115**, 163603 (2015).

[37] See Supplemental Material at http://link.aps.org/supplemental/10.1103/PhysRevResearch.7.L012014 for derivation of the formalism, discussion on decoherence-free subspaces, comparison to reservoir engineering, derivation of the emergent coherent dynamics, details on the adiabatic elimination procedure, details on the dynamics of larger systems, and derivation of the effect of thermal noise.

[38] J. Combes, J. Kerckhoff, and M. Sarovar, The SLH framework for modeling quantum input-output networks, Adv. Phys.: X **2**, 784 (2017).

[39] A. Periwal, E. S. Cooper, P. Kunkel, J. F. Wienand, E. J. Davis, and M. Schleier-Smith, Programmable interactions and emer-

gent geometry in an array of atom clouds, Nature (London) **600**, 630 (2021).

[40] G. Bentsen, T. Hashizume, A. S. Buyskikh, E. J. Davis, A. J. Daley, S. S. Gubser, and M. Schleier-Smith, Treelike interactions and fast scrambling with cold atoms, Phys. Rev. Lett. **123**, 130601 (2019).

[41] J. Ma, X. Wang, C. P. Sun, and F. Nori, Quantum spin squeezing, Phys. Rep. **509**, 89 (2011).

[42] Y. C. Liu, Z. F. Xu, G. R. Jin, and L. You, Spin squeezing: Transforming one-axis twisting into two-axis twisting, Phys. Rev. Lett. **107**, 013601 (2011).

[43] V. V. Albert and L. Jiang, Symmetries and conserved quantities in Lindblad master equations, Phys. Rev. A **89**, 022118 (2014).

[44] A. V. Poshakinskiy and A. N. Poddubny, Dimerization of many-body subradiant states in waveguide quantum electrodynamics, Phys. Rev. Lett. **127**, 173601 (2021).

[45] D. Finkelstein-Shapiro, D. Viennot, I. Saideh, T. Hansen, T. Pullerits, and A. Keller, Adiabatic elimination and subspace evolution of open quantum systems, Phys. Rev. A **101**, 042102 (2020).

[46] A. P. Foster, D. Hallett, I. V. Iorsh, S. J. Sheldon, M. R. Godsland, B. Royall, E. Clarke, I. A. Shelykh, A. M. Fox, M. S. Skolnick, I. E. Itskevich, and L. R. Wilson, Tunable photon statistics exploiting the Fano effect in a waveguide, Phys. Rev. Lett. **122**, 173603 (2019).

[47] M. Mirhosseini, E. Kim, X. Zhang, A. Sipahigil, P. B. Dieterle, A. J. Keller, A. Asenjo-Garcia, D. E. Chang, and O. Painter, Cavity quantum electrodynamics with atom-like mirrors, Nature (London) **569**, 692 (2019).

[48] M. Arcari, I. Söllner, A. Javadi, S. Lindskov Hansen, S. Mahmoodian, J. Liu, H. Thyrrestrup, E. H. Lee, J. D. Song, S. Stobbe, and P. Lodahl, Near-unity coupling efficiency of a quantum emitter to a photonic crystal waveguide, Phys. Rev. Lett. **113**, 093603 (2014).

[49] Z. Wang, S. Shankar, Z. K. Minev, P. Campagne-Ibarcq, A. Narla, and M. H. Devoret, Cavity attenuators for superconducting qubits, Phys. Rev. Appl. **11**, 014031 (2019).

[50] A. Somoroff, Q. Ficheux, R. A. Mencia, H. Xiong, R. Kuzmin, and V. E. Manucharyan, Millisecond coherence in a superconducting qubit, Phys. Rev. Lett. **130**, 267001 (2023).

[51] M. D. Hutchings, J. B. Hertzberg, Y. Liu, N. T. Bronn, G. A. Keefe, M. Brink, J. M. Chow, and B. L. T. Plourde, Tunable superconducting qubits with flux-independent coherence, Phys. Rev. Appl. **8**, 044003 (2017).

[52] J. D. Brehm, A. N. Poddubny, A. Stehli, T. Wolz, H. Rotzinger, and A. V. Ustinov, Waveguide bandgap engineering with an array of superconducting qubits, npj Quantum Mater. **6**, 10 (2021).

[53] A. L. Grimsmo and A. Blais, Squeezing and quantum state engineering with Josephson travelling wave amplifiers, npj Quantum Inf. **3**, 20 (2017).

[54] N. Nishad, A. Keselman, T. Lahaye, A. Browaeys, and S. Tsesses, Quantum simulation of generic spin-exchange models in Floquet-engineered Rydberg-atom arrays, Phys. Rev. A **108**, 053318 (2023).

[55] I. Hurvitz, A. Arie, and A. Karnieli, Frequency-domain engineering of bright squeezed vacuum for continuous-variable quantum information, Opt. Express **31**, 20387 (2023).

[56] M. F. Yanik, W. Suh, Z. Wang, and S. Fan, Stopping light in a waveguide with an all-optical analog of electromagnetically induced transparency, Phys. Rev. Lett. **93**, 233903 (2004).

[57] M. Zanner, R. Albert, E. I. Rosenthal, S. Casulleras, I. Yang, C. M. F. Schneider, O. Romero-Isart, and G. Kirchmair, Spatial addressing of qubits in a dispersive waveguide, arXiv:2407.10617.

[58] T. Shi and S. Fan, Two-photon transport through a waveguide coupling to a whispering-gallery resonator containing an atom and photon-blockade effect, Phys. Rev. A **87**, 063818 (2013).

[59] T. Shi, Y. Chang, and J. J. García-Ripoll, Ultrastrong coupling few-photon scattering theory, Phys. Rev. Lett. **120**, 153602 (2018).

[60] Y. Ke, A. V. Poshakinskiy, C. Lee, Y. S. Kivshar, and A. N. Poddubny, Inelastic scattering of photon pairs in qubit arrays with subradiant states, Phys. Rev. Lett. **123**, 253601 (2019).

[61] Z. Wang, T. Jaako, P. Kirton, and P. Rabl, Supercorrelated radiance in nonlinear photonic waveguides, Phys. Rev. Lett. **124**, 213601 (2020).

[62] X. Wang, J.-Q. Li, T. Liu, A. Miranowicz, and F. Nori, Long-range four-body interactions in structured nonlinear photonic waveguides, Phys. Rev. Res. **6**, 043226 (2024).

[63] L. L. Wan and X. Y. Lü, Quantum-squeezing-induced point-gap topology and skin effect, Phys. Rev. Lett. **130**, 203605 (2023).

[64] M. A. Perlin, C. Qu, and A. M. Rey, Spin squeezing with short-range spin-exchange interactions, Phys. Rev. Lett. **125**, 223401 (2020).

[65] Y. Lu, N. Lambert, A. F. Kockum, K. Funo, A. Bengtsson, S. Gasparinetti, F. Nori, and P. Delsing, Steady-state heat transport and work with a single artificial atom coupled to a waveguide: Emission without external driving, PRX Quantum **3**, 020305 (2022).

[66] J. Q. Quach and W. J. Munro, Using dark states to charge and stabilize open quantum batteries, Phys. Rev. Appl. **14**, 024092 (2020).